ACS Macro Letters

Letter

pubs.acs.org/macroletters

Three-Phase Morphology of Semicrystalline Polymer Semiconductors: A Quantitative Analysis

Roddel Remy,[†] Sujun Wei,[‡,§] Luis M. Campos,[‡] and Michael E. Mackay*[,†,∥]

Departments of [†]Materials Science and Engineering and [∥]Chemical and Biomolecular Engineering, University of Delaware, Newark, Delaware, United States

[‡]Department of Chemistry, Columbia University, New York New York United States

Supporting Information

ABSTRACT: Quantitative morphological analysis is essential to the fundamental understanding of semiconducting polymers. Temperature modulated differential scanning calorimetry is used to determine the amount of crystalline and noncrystalline phases within regioregular poly(3-hexylthiophene) (rrP3HT). Careful optimization of the experimental conditions shows that the glass transition of rrP3HT consists of three parts corresponding to the devitrification of the side chains, mobile amorphous fraction (MAF), and rigid amorphous fraction (RAF), consecutively. Measurements taken from this, as well as from the melting transition, allows the first calculation of the degree of crystallinity, MAF and RAF, to be achieved in a single experiment for rrP3HT. This technique thus enables the morphological phases to be determined and potentially related to the performance of electronic devices made from semiconducting polymers.

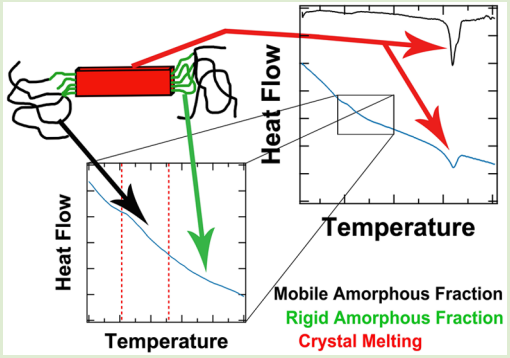

Semiconducting polymers have shown great utility in applications such as field effect transistors, light emitting diodes and solar cells. Poly(alkylthiophene)s, especially poly(3-hexylthiophene) (P3HT), are the most widely investigated polymers for these applications, but the performance of these materials is highly dependent on their morphology. Regioregular P3HT (rrP3HT) is a semicrystalline polymer and it has been shown[1] that its crystallinity is important in determining its electrical properties, which directly influences device performance; a classic materials science challenge to relate morphology to performance.

The most facile method of determining quantitative polymer crystallinity is via differential scanning calorimetry (DSC). All that is required is knowledge of the enthalpy of fusion of an infinitely large crystal (ΔH_m^∞) for the polymer in question. For some time there has been conflict in the literature about this value for rrP3HT.[2−5] Recently, though, we have determined ΔH_m^∞ = 42.9 J/g for rrP3HT using an approach derived from the literature on linear polyethylene[6] that agrees well with the value given by Snyder et al.[7] Now it is possible to quantitatively determine the crystallinity of a P3HT specimen using DSC to address the above challenge.

While polymer crystallinity is important, it has also been shown that more attention should be directed to the disordered or amorphous component of these materials.[8−15] It is well-known that the hole mobility for rrP3HT and other semiconducting polymers, by extension, increases with molecular weight.[8−13] The reason is due to an increase in the number of entanglements so the material consists of crystallites that are interconnected by amorphous chain segments spanning them (also known as tie chains). This point was expounded upon further by Noriega et al. who discovered that the measured paracrystallinity (or degree of disorder) in these materials is correlated to their charge transport properties and that poorly ordered materials have a tolerance to charge traps within aggregates.[14] Utilizing cyclic voltammetry, UV−vis absorption, and ultraviolet photoelectron spectroscopy, Sweetnam et al. observed valence band offsets between amorphous and crystalline portions of semiconducting polymers and blends containing a fullerene donor that acts as a driving force for hole extraction from the mixed phase, thereby improving charge separation.[15] Due to the importance of morphological details to charge transport properties, we present a method that provides quantitative data representing the physical fractions of crystalline and amorphous material present in rrP3HT to deepen the understanding of the multiphase morphology of semiconducting polymers.

From the polymer physics perspective, the amorphous polymer phase can be further divided into two fractions. The first fraction consists of the traditional amorphous chains, where they are free to move according to the standard polymer kinetics models above the glass transition temperature (T_g). This is called the mobile amorphous fraction (MAF). The second fraction consists of constrained, yet still disordered,

Received: July 14, 2015
Accepted: August 21, 2015
Published: September 2, 2015

DOI: 10.1021/acsmacrolett.5b00481
ACS Macro Lett. 2015, 4, 1051−1055

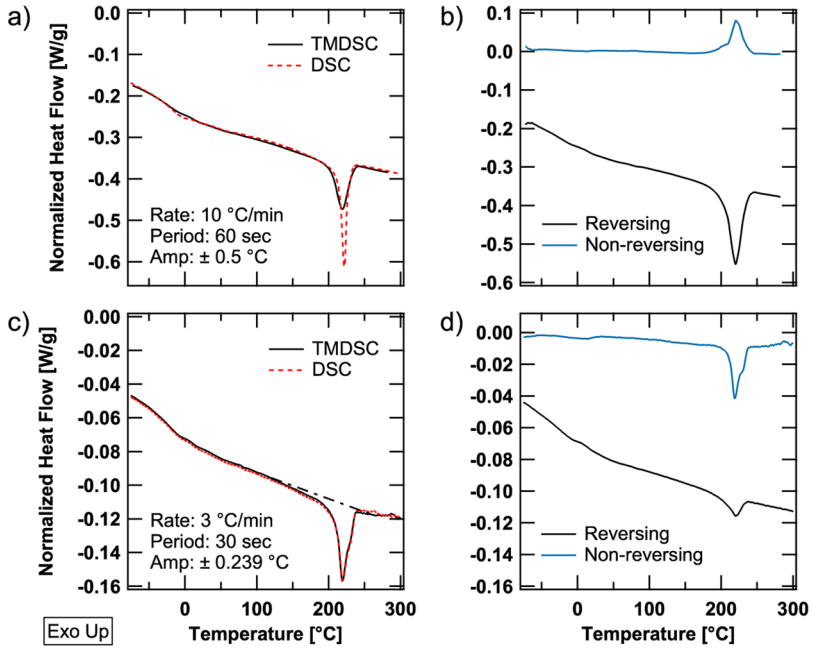

Figure 1. Deconvoluted data from two TMDSC experiments on rrP3HT. Total heat flow thermograms are shown in (a) and (c) with their experimental parameters. An overlay of their respective heat flow signals from a typical DSC experiment (red dashed lines) is also shown to illustrate the similarity in the resultant data of both methods. Black dot-dashed line in (c) defines the area used to calculate sample crystallinity. Reversing and nonreversing heat flow thermograms for (a) and (c) are displayed in (b) and (d), respectively.

chains called the rigid amorphous fraction (RAF). These terms were first coined by Wunderlich and co-workers while investigating the glass transition of poly(oxymethylene).[16] RAF has since been discovered in many other semicrystalline polymers[17] and is thought to exist at crystal/amorphous interfaces as well as interfaces between polymers and fillers in composites.[18,19] With regard to semiconducting polymers, there has been literature mentioning its existence, mainly in relation to anomalies or deviations in data sets, although the quantity present was not determined.[2,20−24]

Temperature-modulated DSC (TMDSC) has been previously proven effective at elucidating the weak T_g of rrP3HT and has been used to construct phase diagrams of rrP3HT and fullerene mixtures.[25−27] Here, TMDSC is utilized to examine rrP3HT samples for the presence of all three polymer phases defined above. First, we describe the TMDSC criteria for accurate data collection which allows for a comprehensive analysis in one experiment. The step change in heat capacity at T_g ($\Delta C_{p,amor}$) for fully amorphous regiorandom P3HT (ranP3HT) is then evaluated for use in determining the RAF. By focusing on the T_g of rrP3HT, analysis can be performed to properly elucidate its nature as a three-step transition, which involves the devitrification of different parts of the polymer chain in sequence. Finally, the first calculation of rrP3HT MAF and RAF in the literature to date is accomplished.

Experiments in this report were performed on rrP3HT purchased from Luminescence Technologies Corp ($M_w \sim 45$ kg/mol, PDI > 2, regioregularity >95%) and were used without further purification. ranP3HT also employed here was synthesized according to the literature[28] (M_n = 21.6 kg/mol, PDI = 2.0, and 56% H−T coupling, determined by NMR). DSC measurements were done at 10 °C/min and TMDSC measurement parameters are displayed in the respective figures below. Before testing, rrP3HT specimens were first crystallized from the melt at 10 °C/min to impart identical thermal histories, while ranP3HT samples were quenched from 300 °C to preserve its amorphous nature.

While typical DSC has only one parameter, the heating rate (b in °C/min), TMDSC has three, the heating rate (b), the amplitude of modulation (B in °C), and the period of modulation (p in sec), each of which affects the data output according to the relation:

$$T(t) = T_0 + bt + B \sin\left(\frac{2\pi}{p}t\right) \quad (1)$$

where $T(t)$ is the temperature at a given time t and T_0 is the initial temperature. Full mathematical descriptions of TMDSC have been published elsewhere.[29,30] Moreover, the method by which data is extracted involves a deconvolution procedure (in most cases a Fourier Transform), which requires sufficient oscillations within a given transition to produce a correct result with a satisfactorily small error. Therefore, to obtain the most accurate information from TMDSC, the experimental parameters must be optimized.

To this end, we refer to the early work of Reading and co-workers.[31−33] They showed that TMDSC is virtually indistinguishable from conventional DSC of the same heating rate by overlaying the total heat flow from TMDSC and the heat flow from conventional DSC.[33] It was also illustrated that there is little loss of quantitative information with a change in experimental method. Figure 1 displays this overlay plot for rrP3HT with two different TMDSC parameter sets. The parameters for Figure 1a,b were obtained from recent literature,[24] while Figure 1c,d are the parameters employed in the present study. Clearly, the experimental conditions used to produce the data in Figure 1c are in agreement with the expected result.

A difference in the data is also observed in the reversing and nonreversing signals. In fact, another requirement mentioned by Reading and co-workers is the necessity for multiple

DOI: 10.1021/acsmacrolett.5b00481
ACS Macro Lett. 2015, 4, 1051−1055

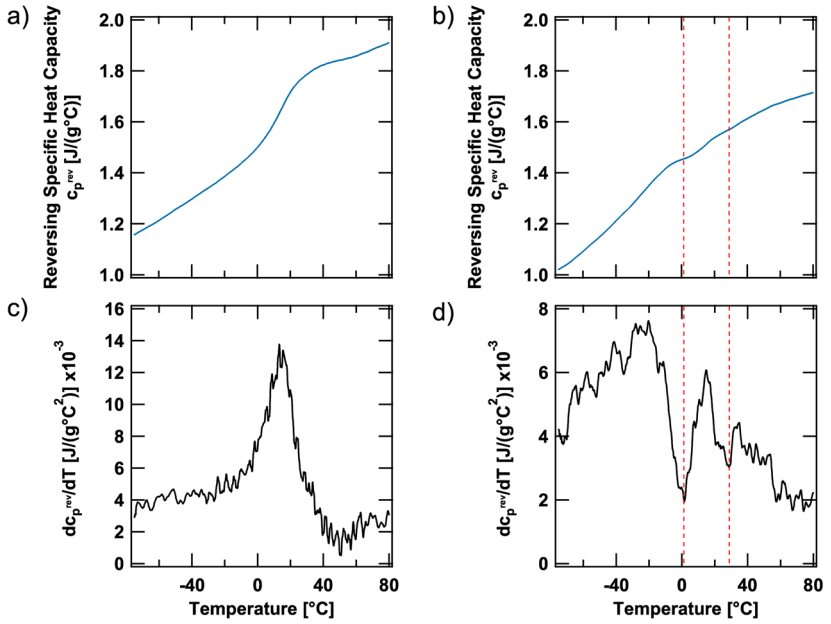

Figure 2. TMDSC thermograms showing c_p^{rev} of ranP3HT (a) and rrP3HT (b), along with their respective derivatives, dc_p^{rev}/dT, in (c) and (d). The red dashed lines in (b) and (d) identify the local minima in dc_p^{rev}/dT for rrP3HT used to assign regions I, II, and III.

Table 1. Measurements from TMDSC of rrP3HT

	crystalline fraction	MAF	RAF
measured values	ΔH_m = 18.0 J/g	$\Delta C_{p,1}$ = 0.097 J/g °C	$\Delta C_{p,2}$ = 0.081 J/g °C
calculated percentage	42.0%	30.3%	25.3%

temperature oscillations over a given transition, such as the melting point (achieved by lowering the heating rate and period of oscillation), which reduces the deconvolution error associated with the analysis.[31−33] While it could be said that Figure 1b shows recrystallization and reorganization during melting, the incorrect parameters and low oscillation density across the melting transition render this description false (see Supporting Information). Figure 1d correctly shows the bulk of the melting process occurring in the nonreversing signal since melting should not follow the applied temperature oscillations. We contend, therefore, that care must be taken in the choice of TMDSC experimental parameters, and the results of Beckingham et al.[24] may require additional evidence to properly support their claim.

In addition to the stated TMDSC requirements, to obtain quantitative crystallinity measurements, the sample should not be allowed to cool (and therefore crystallize) during the experiment. Thus, the oscillation amplitude was reduced to where the instantaneous heating rate is never negative (i.e., $dT(t)/dt \geq 0$). The technique utilizing this restriction is called heat-only TMDSC and is applied to all subsequent data shown in this work.

The rigid amorphous fraction (RAF) is calculated according to the equation:[16,17]

$$\mathrm{RAF} = 1 - \frac{\Delta H_m}{\Delta H_m^{\infty}} - \frac{\Delta C_{p,sam}}{\Delta C_{p,amor}} \quad (2)$$

where ΔH_m is the sample enthalpy of melting, ΔH_m^{∞} is the enthalpy of fusion of a perfect, infinite P3HT crystal, $\Delta C_{p,sam}$ is the step change in heat capacity at T_g of the sample and $\Delta C_{p,amor}$ is the step change in heat capacity at T_g of 100% amorphous P3HT. The second term in eq 2 is the sample's crystallinity and the final term is its MAF. We have previously determined ΔH_m^{∞} for rrP3HT[6] and ΔH_m is directly measured from the total heat flow data (or the sum of the reversing and nonreversing melting transitions, whichever is easier; see Figure 1). However, the final term (or MAF) of the expression has never been evaluated for P3HT.

While it is difficult to obtain 100% amorphous rrP3HT, ranP3HT is naturally amorphous and of identical chemical composition. Therefore, $\Delta C_{p,amor}$ can be directly measured from the T_g of ranP3HT, as depicted in Figure 2. From the derivative curve (Figure 2c) it is obvious that the T_g of ranP3HT is one single transition at 15 °C and a value of $\Delta C_{p,amor}$ = 0.32 ± 0.02 J/g °C is obtained. According to Wunderlich's calculations,[34] approximately five "mobile beads" within the monomer unit contribute to $\Delta C_{p,amor}$ for P3HT (see Supporting Information). In contrast, the T_g and derivative curve of rrP3HT, shown in Figure 2b and d, respectively, is more complicated.

First, there is a transition that culminates at approximately 0 °C but extends to temperatures below the instrument's capabilities. Previous research has described that this is likely from configurational dynamics of the side chains[23] with an onset just before −75 °C.[22] Interestingly, this is not noticeable in ranP3HT, suggesting that it may originate from the side chains within the crystallites, but confirmation of this is beyond the scope of this paper. Immediately afterward, the T_g of the polymer occurs, so the measurement of $\Delta C_{p,sam}$ for rrP3HT was first taken between 0 and 65 °C, where the derivative curve plateaus (see Figure 2c). It should be mentioned that no side chain melting was observed in this experiment, as was seen for lower molecular weight rrP3HT[3,35,36] (see Figure 1d). With all

DOI: 10.1021/acsmacrolett.5b00481
ACS Macro Lett. 2015, 4, 1051−1055

of the necessary information, the resultant RAF for rrP3HT is ≈2%.

Yet, this value is uncharacteristically low for a polymer with such high crystallinity (see Table 1). Reconsidering the derivative curve for rrP3HT reveals the T_g as a two-step transition evidenced by the minimum in the derivative at ≈30 °C (see Figure 2d). In this light, an alternate calculation was performed whereby $\Delta C_{p,sam}$ was divided into $\Delta C_{p,1}$ and $\Delta C_{p,2}$, as shown in Figure 3, to represent the devitrification of the

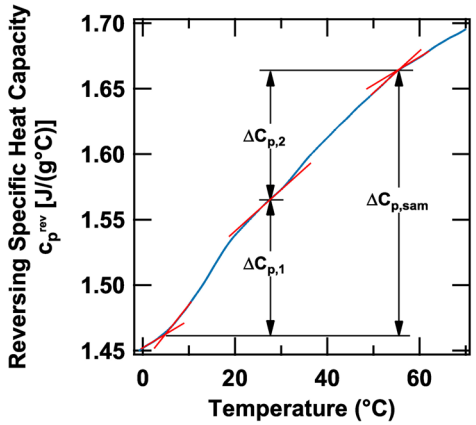

Figure 3. Closer view of c_p^{rev} of rrP3HT showing how $\Delta C_{p,sam}$ was split into $\Delta C_{p,1}$ and $\Delta C_{p,2}$ for the calculation of MAF and RAF, respectively.

MAF then RAF successively. Since $\Delta C_{p,1}$ occurs in the same location as the fully mobile ranP3HT T_g, this transition is due to the MAF, which means $\Delta C_{p,2}$ is therefore the relaxation of the RAF in rrP3HT. By dividing $\Delta C_{p,1}$ and $\Delta C_{p,2}$ by $\Delta C_{p,amor}$, the mass percentages of MAF and RAF were found, respectively, and are shown in Table 1. (One can also use $\Delta C_{p,1}$ as $\Delta C_{p,sam}$ in eq 2 to obtain a similar RAF to Table 1. The similar result from both methods validates the assignment of $\Delta C_{p,2}$ as the RAF transition.) Finally, a summation of all three phases gives 97.6% that, although less than 100%, is accurate considering the error in $\Delta C_{p,amor}$ is ≈6%. These results are comparable with calculations performed on other semicrystalline polymers.[16]

The RAF calculated here represents at least a fraction of the tie molecules and dangling chain ends that protrude from the rrP3HT crystallites formed from the nonisothermal crystallization preformed prior to data collection, as was described earlier. This would be the only location where amorphous polymer chains are under constraint in this experiment. Due to this, the RAF is potentially an essential part of the charge transfer interface between crystalline and amorphous polymer regions (i.e., MAF) or between crystallites and fullerene aggregates in solar cells. Research into other sources of, and changes in, RAF in semiconducting polymers due to processing and electronic device fabrication is ongoing.

In conclusion, it has been found that the amorphous regions of rrP3HT relax before a rather modest 65 °C, well below typical P3HT annealing temperatures (120−140 °C). The result not only represents the first quantification of these morphological entities in rrP3HT, but also has implications in the description of the charge transfer interface in electronic devices made from it. Additionally, many of the high performance semiconducting polymers being studied currently are completely amorphous, which places even more importance on the MAF and RAF that are formed in these systems. Hence, quantitative research into the disordered phases of polymer semiconductors will deepen the understanding of the morphology necessary to optimize electronic device performance.

■ ASSOCIATED CONTENT

Supporting Information

The Supporting Information is available free of charge on the ACS Publications website at DOI: 10.1021/acsmacrolett.5b00481.

Modulated heat flow data and calculation and proposed assignment of "mobile beads" to P3HT monomer (PDF)

■ AUTHOR INFORMATION

Corresponding Author

*E-mail: mem@udel.edu.

Present Address

§Department of Chemistry, Queensborough Community College, Bayside NY, U.S.A.

Notes

The authors declare no competing financial interest.

■ ACKNOWLEDGMENTS

The authors thank the University of Delaware for funding and support of this research, as well as NIST through award 70NANOBIOH256, through the Center for Neutron Science at the University of Delaware.

■ REFERENCES

(1) van Bavel, S. S.; Bärenklau, M.; de With, G.; Hoppe, H.; Loos, J. *Adv. Funct. Mater.* **2010**, *20*, 1458−1463.
(2) Malik, S.; Nandi, A. K. *J. Polym. Sci., Part B: Polym. Phys.* **2002**, *40*, 2073−2085.
(3) Pascui, O. F.; Lohwasser, R.; Sommer, M.; Thelakkat, M.; Thurn-Albrecht, T.; Saalwachter, K. *Macromolecules* **2010**, *43*, 9401−9410.
(4) Balko, J.; Lohwasser, R. H.; Sommer, M.; Thelakkat, M.; Thurn-Albrecht, T. *Macromolecules* **2013**, *46*, 9642−9651.
(5) Lee, C. S.; Dadmun, M. D. *Polymer* **2014**, *55*, 4−7.
(6) Remy, R.; Weiss, E. D.; Nguyen, N. A.; Wei, S.; Campos, L. M.; Kowalewski, T.; Mackay, M. E. *J. Polym. Sci., Part B: Polym. Phys.* **2014**, *52*, 1469−1475.
(7) Snyder, C. R.; Nieuwendaal, R. C.; DeLongchamp, D. M.; Luscombe, C. K.; Sista, P.; Boyd, S. D. *Macromolecules* **2014**, *47*, 3942−3950.
(8) Kline, R.; McGehee, M.; Kadnikova, E.; Liu, J.; Fréchet, J. *Adv. Mater.* **2003**, *15*, 1519−1522.
(9) Kline, R.; McGehee, M.; Kadnikova, E.; Liu, J.; Frechet, J. M.; Toney, M. F. *Macromolecules* **2005**, *38*, 3312−3319.
(10) Zhang, R.; Li, B.; Iovu, M. C.; Jeffries-El, M.; Sauvé, G.; Cooper, J.; Jia, S.; Tristram-Nagle, S.; Smilgies, D. M.; Lambeth, D. N.; McCullough, R. D.; Kowalewski, T. *J. Am. Chem. Soc.* **2006**, *128*, 3480−3481.
(11) Chang, J.-F.; Clark, J.; Zhao, N.; Sirringhaus, H.; Breiby, D. W.; Andreasen, J. W.; Nielsen, M. M.; Giles, M.; Heeney, M.; McCulloch, I. *Phys. Rev. B: Condens. Matter Mater. Phys.* **2006**, *74*, 115318.
(12) Virkar, A. A.; Mannsfeld, S.; Bao, Z.; Stingelin, N. *Adv. Mater.* **2010**, *22*, 3857−75.
(13) Koch, F. P. V.; et al. *Prog. Polym. Sci.* **2013**, *38*, 1978−1989.
(14) Noriega, R.; Rivnay, J.; Vandewal, K.; Koch, F. P. V.; Stingelin, N.; Smith, P.; Toney, M. F.; Salleo, A. *Nat. Mater.* **2013**, *12*, 1038−44.
(15) Sweetnam, S.; Graham, K. R.; Ngongang Ndjawa, G. O.; Heumüller, T.; Bartelt, J. A.; Burke, T. M.; Li, W.; You, W.; Amassian, A.; McGehee, M. D. *J. Am. Chem. Soc.* **2014**, *136*, 14078−88.
(16) Suzuki, H.; Grebowicz, J.; Wunderlich, B. *Br. Polym. J.* **1985**, *17*, 1−3.

DOI: 10.1021/acsmacrolett.5b00481
ACS Macro Lett. 2015, 4, 1051−1055

(17) Wunderlich, B. *Prog. Polym. Sci.* **2003**, *28*, 383−450.
(18) Sargsyan, A.; Tonoyan, A.; Davtyan, S.; Schick, C. *Eur. Polym. J.* **2007**, *43*, 3113−3127.
(19) Wurm, A.; Ismail, M.; Kretzschmar, B.; Pospiech, D.; Schick, C. *Macromolecules* **2010**, *43*, 1480−1487.
(20) Lu, S. X.; Cebe, P. *J. Appl. Polym. Sci.* **1996**, *61*, 473−483.
(21) Pal, S.; Nandi, A. K. *Polymer* **2005**, *46*, 8321−8330.
(22) Pankaj, S.; Hempel, E.; Beiner, M. *Macromolecules* **2009**, *42*, 716−724.
(23) Nieuwendaal, R. C.; Snyder, C. R.; DeLongchamp, D. M. *ACS Macro Lett.* **2014**, *3*, 130−135.
(24) Beckingham, B. S.; Ho, V.; Segalman, R. A. *ACS Macro Lett.* **2014**, *3*, 684−688.
(25) Zhao, J.; Swinnen, A.; Van Assche, G.; Manca, J.; Vanderzande, D.; Van Mele, B. *J. Phys. Chem. B* **2009**, *113*, 1587−91.
(26) Zhao, J.; Bertho, S.; Vandenbergh, J.; Van Assche, G.; Manca, J.; Vanderzande, D.; Yin, X.; Shi, J.; Cleij, T.; Lutsen, L.; Van Mele, B.; Assche, G. V.; Mele, B. V. *Phys. Chem. Chem. Phys.* **2011**, *13*, 12285−92.
(27) Ngo, T. T.; Nguyen, D. N.; Nguyen, V. T. *Adv. Nat. Sci.: Nanosci. Nanotechnol.* **2012**, *3*, 045001.
(28) McCullough, R. D. *Adv. Mater.* **1998**, *10*, 93−116.
(29) Wunderlich, B.; Jin, Y.; Boller, A. *Thermochim. Acta* **1994**, *238*, 277−293.
(30) Lacey, A. A.; Nikolopoulos, C.; Reading, M. *J. Therm. Anal.* **1997**, *50*, 279−333.
(31) Gill, P. S.; Sauerbrunn, S. R.; Reading, M. *J. Therm. Anal.* **1993**, *40*, 931−939.
(32) Reading, M.; Elliott, D.; Hill, V. L. *J. Therm. Anal.* **1993**, *40*, 949−955.
(33) Reading, M. *Trends Polym. Sci.* **1993**, *1*, 248−253.
(34) Wunderlich, B. *J. Phys. Chem.* **1960**, *64*, 1052−1056.
(35) Wu, Z.; Petzold, A.; Henze, T.; Thurn-Albrecht, T.; Lohwasser, R. H.; Sommer, M.; Thelakkat, M. *Macromolecules* **2010**, *43*, 4646−4653.
(36) Yuan, Y.; Zhang, J.; Sun, J.; Hu, J.; Zhang, T.; Duan, Y. *Macromolecules* **2011**, *44*, 9341−9350.

DOI: 10.1021/acsmacrolett.5b00481
ACS Macro Lett. 2015, 4, 1051−1055